Electronic Supplementary Information

MOF-on-MOF robust heterostructures as an efficient cathode candidate for next-generation supercapacitor

Rakesh Deka[a], Viresh Kumar[a], and Shaikh M Mobin[a,b,c*]

[a]Department of Chemistry, [b]Center for Electric Vehicle and Intelligent Transport System (CEVIT), [c]Center of Advanced Electronics (CAE), Indian Institute of Technology Indore, Khandwa Road, Simrol, Indore 453552, India.

Corresponding Author: E-mail: xray@iiti.ac.in Tel: +91 731 6603 336

Physical Measurements

All the reagents and solvents were purchased from a commercial source without further purification. Thermogravimetric analysis (TGA) was recorded with a METTLER TOLEDO (TGA/DSC1) system through STARe software by a heating rate of 10 ° C/min in an N_2 atmosphere up to 800° C. For the Powder X-ray diffraction (PXRD) analysis, Cu Kα (0.154 nm) monochromatic radiation was used with a Bruker, D2-Phaser X-ray diffractometer. The morphologies were investigated by a Supra55 Zeiss field emission scanning electron microscope (FESEM), and JEOL microscope with model number JEM 2100F operated on 200 kV voltage has been used to record tunneling electron microscope (TEM) images. Brunauer−Emmett−Teller (BET) surface area and Barrett−Joyner−Halenda (BJH) distribution determinations were conducted on an Autosorb iQ (Quantachrome Instruments, version 1.11). FT-IR experiment was performed by using Perkin Elmer-Spectrum Two with ATR mode. X-ray photoelectron spectroscopic (XPS) analysis (XPS, Nexsa, Thermofisher Scientific) incorporating Al Kα as the source of X-ray.

Electrochemical study

Preparation of electrodes

To evaluate the efficiency of **Ni-BTC@ZIF-67**, electrochemical measurements were conducted using techniques such as potentiostatic cyclic voltammetry (CV), electrochemical impedance spectroscopy (EIS), and galvanostatic charge-discharge (GCD). The setup for these measurements includes three standard electrode systems: consisting of a counter electrode made of platinum wire, a reference electrode made of Ag/AgCl, and a working electrode made of carbon cloth (CC). To prepare the working electrode, a dispersion of the active material in ethanol was drop-cast onto the CC and air-dried at room temperature, with a mass loading of 500 μg, for further electrochemical study.

Efficiency evaluation

The C_s (F g^{-1}) of the symmetric device was measured by using the following equation:[1]

$$C_s = \frac{I \times \Delta t}{m \times \Delta V} \quad \text{(S1)}$$

here *I/m* signifies current density, Δt, and ΔV convey the discharge time and potential window of the GCD profile.

Moreover, the specific capacity (mA h^{-1}) is also estimated from the GCD profile by using the following equation:[2]

$$C_s = \frac{I}{m} \int V dt \quad \text{(S2)}$$

here, I/m signifies current density, and $\int V dt$ signify the area under the discharge curve of the GCD curve.

In the case of the asymmetric supercapacitor device, the energy density (E) and power density (P) were determined using the following equations:[1]

$$E = \frac{Cs}{2 \times 3.6} \times \Delta V^2 \tag{S3}$$

$$P = \frac{E}{\Delta t} \times 3600 \tag{S4}$$

here, C_s signifies specific capacitance, ΔV signifies potential window, and Δt signifies discharge time of the GCD profile, respectively.

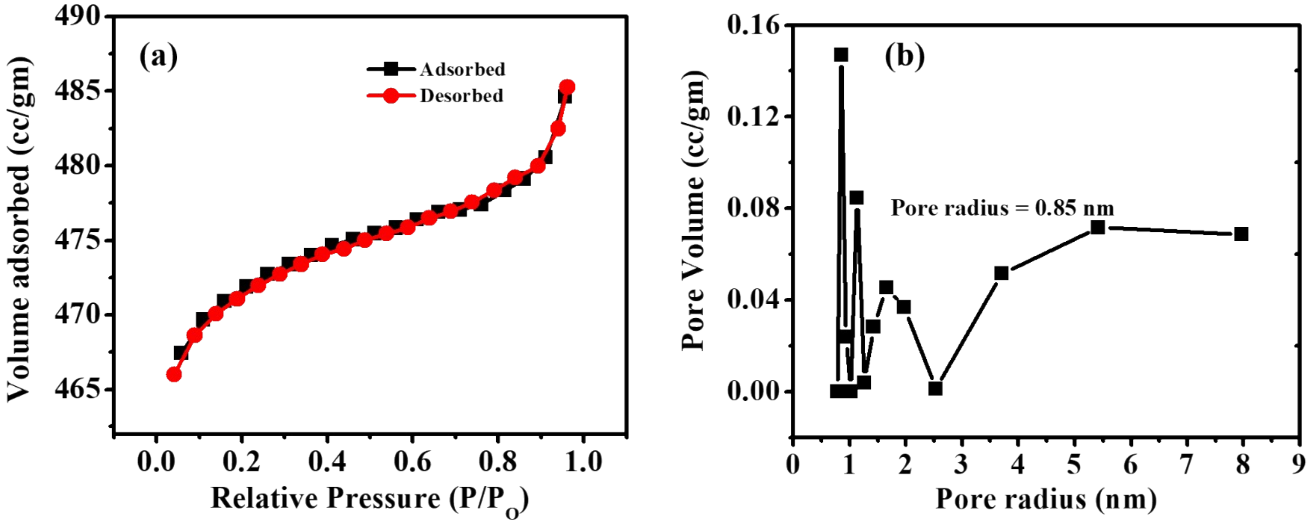

Fig. S1 (a) BET curve, and (b) Pore size distribution of ZIF-67.

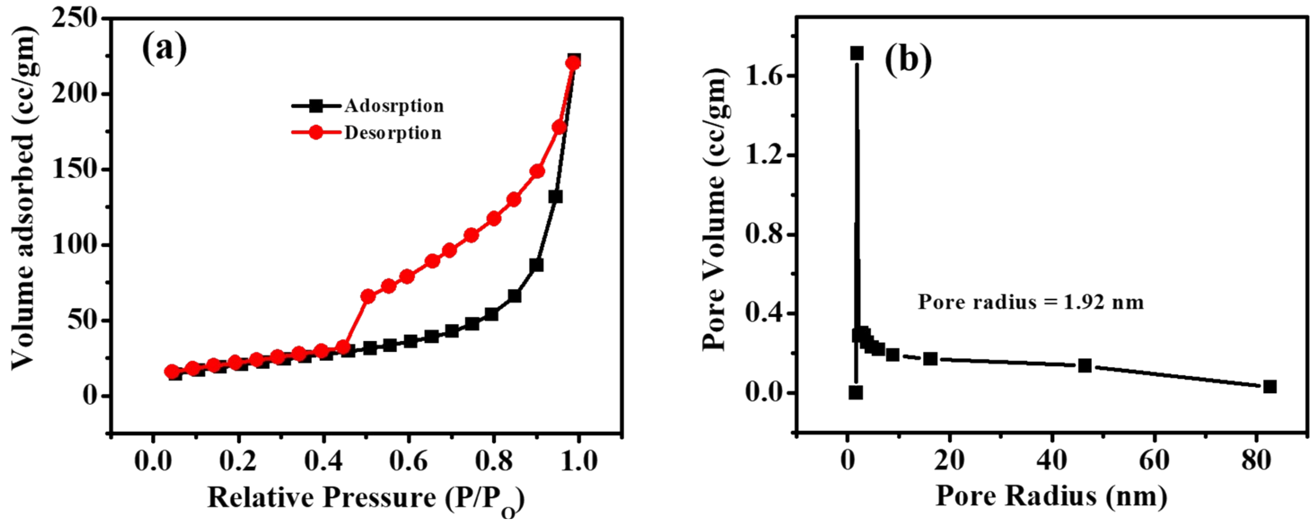

Fig. S2 (a) BET curve, and (b) Pore size distribution of Ni-BTC.

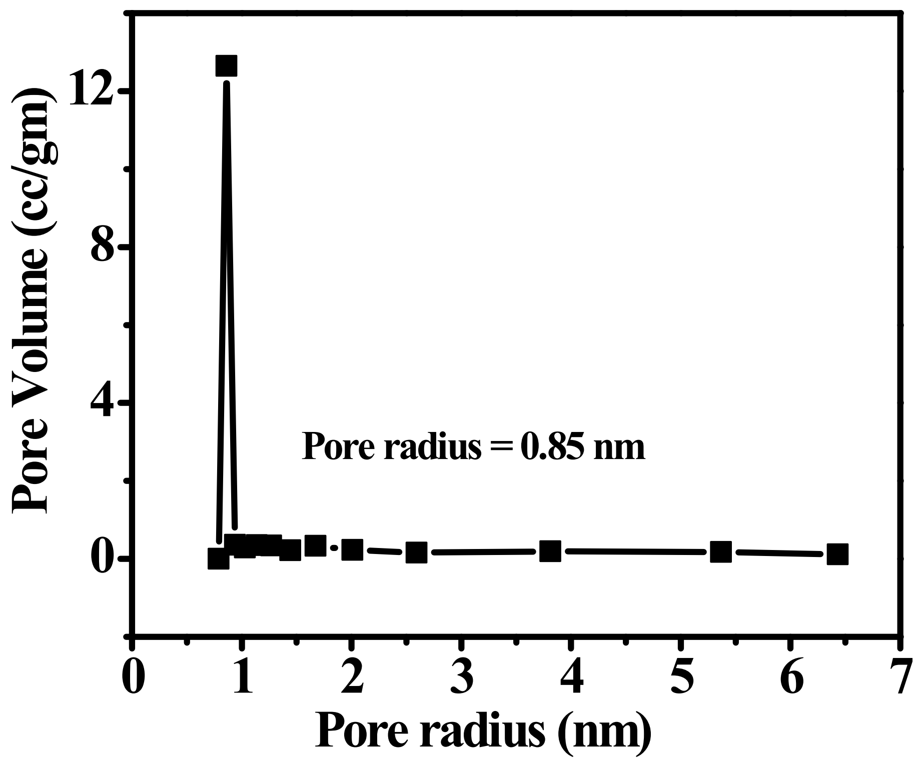

Fig. S3 Pore size distribution curve of **Ni-BTC@ZIF-67.**

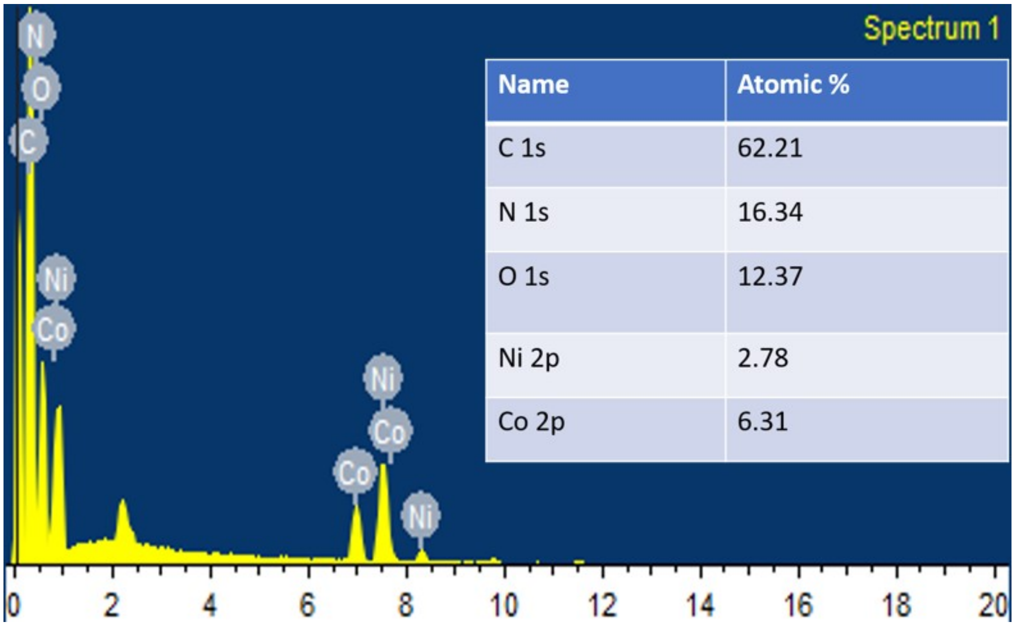

Fig. S4 Elemental composition of **Ni-BTC@ZIF-67**.

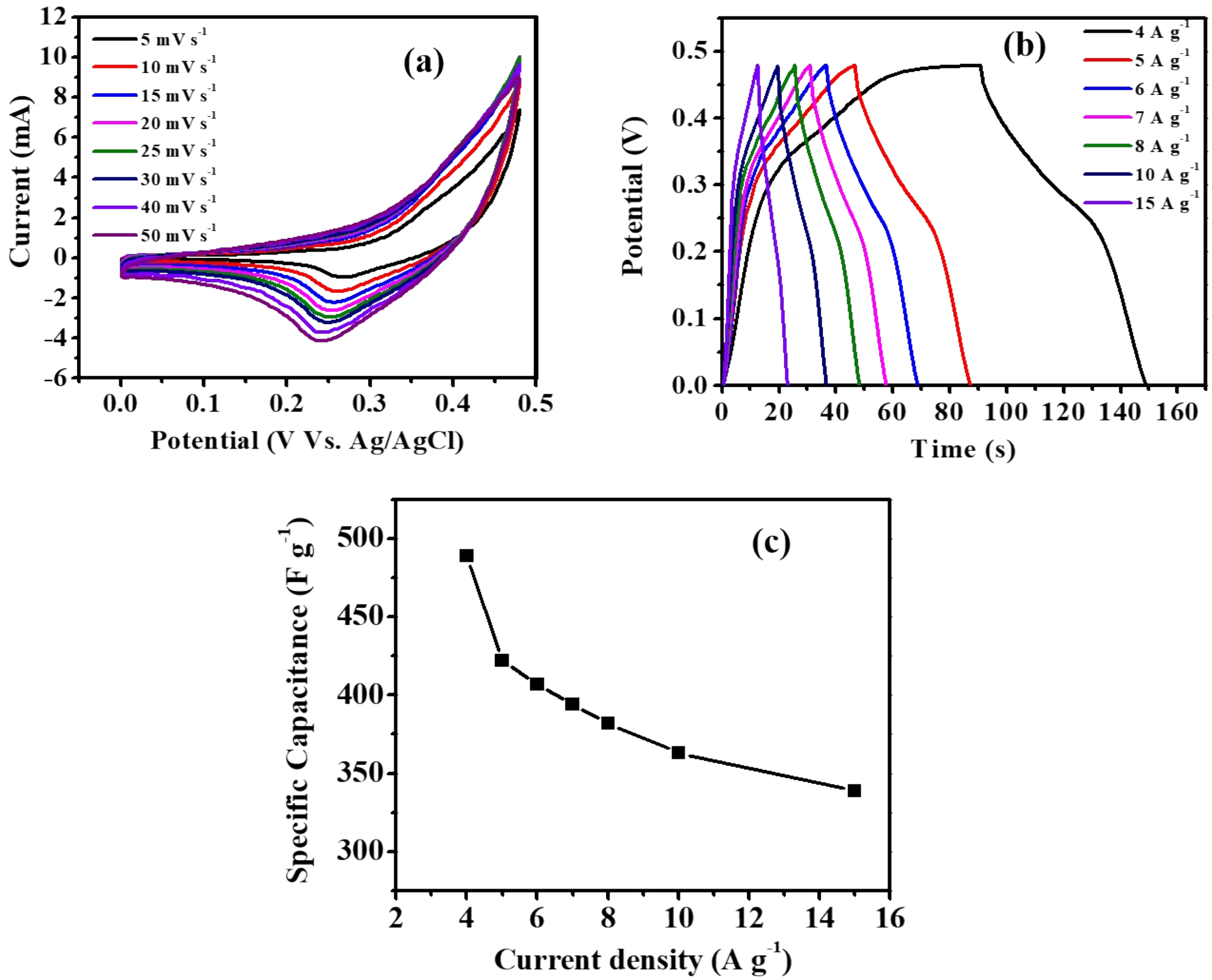

Fig. S5 (a) CV plot at various scan rates, (b) GCD plot at various current densities, and (c) Specific capacitance vs Current density plot of ZIF-67.

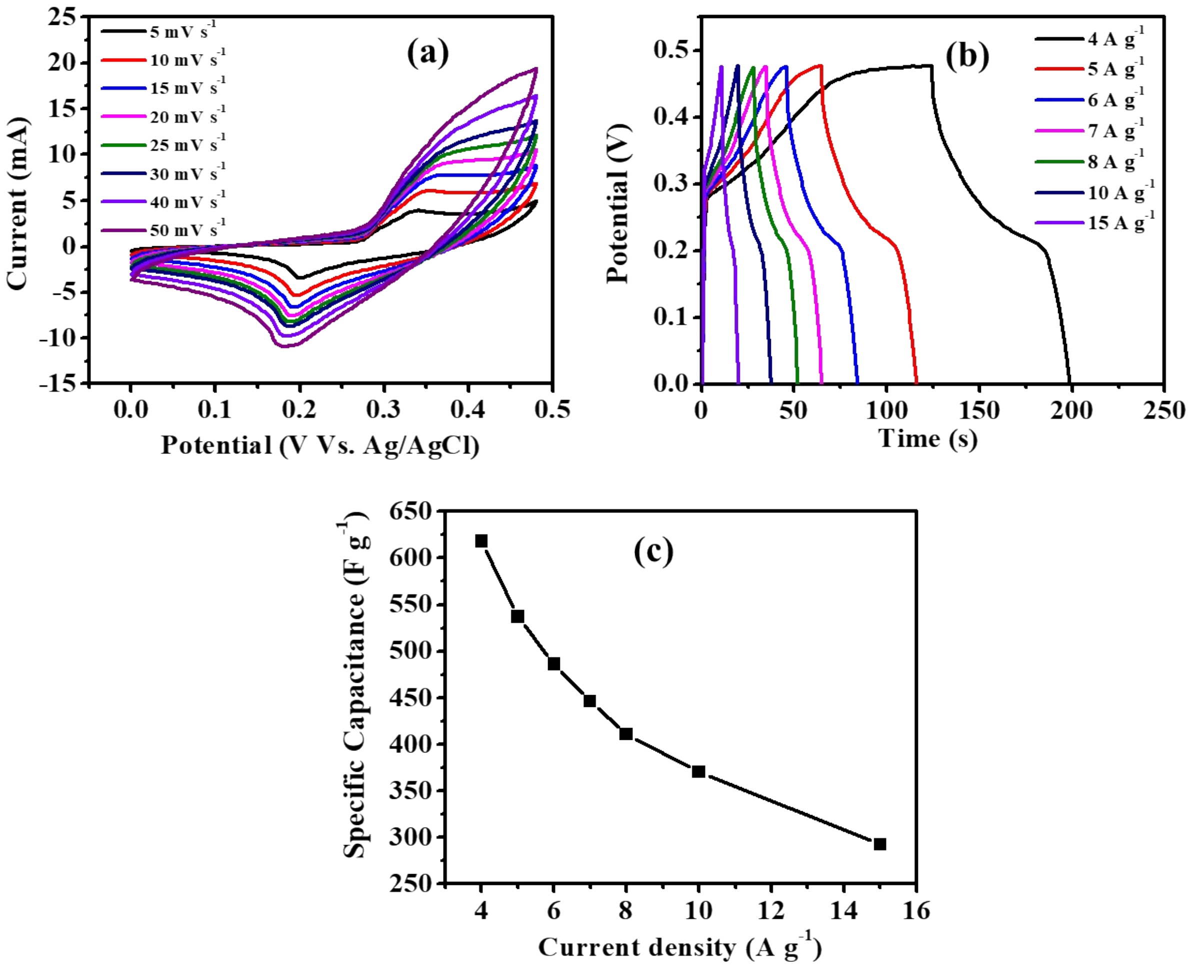

Fig. S6 (a) CV plot at various scan rates, (b) GCD plot at various current densities, and (c) Specific capacitance vs Current density plot of Ni-BTC.

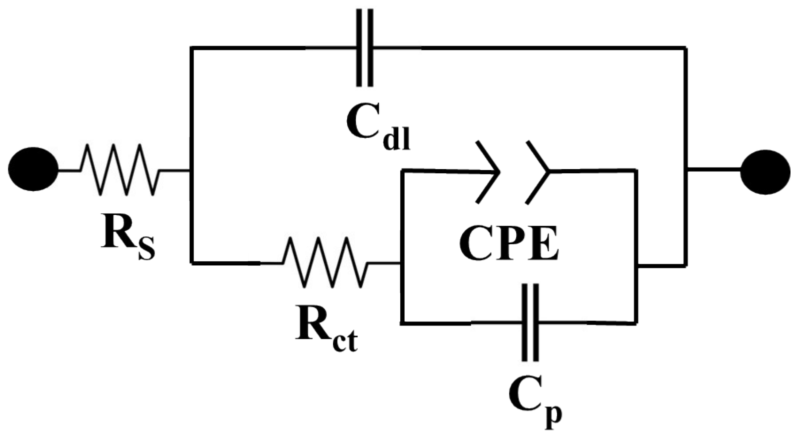

Fig. S7 Equivalent circuit diagram for three electrode system.

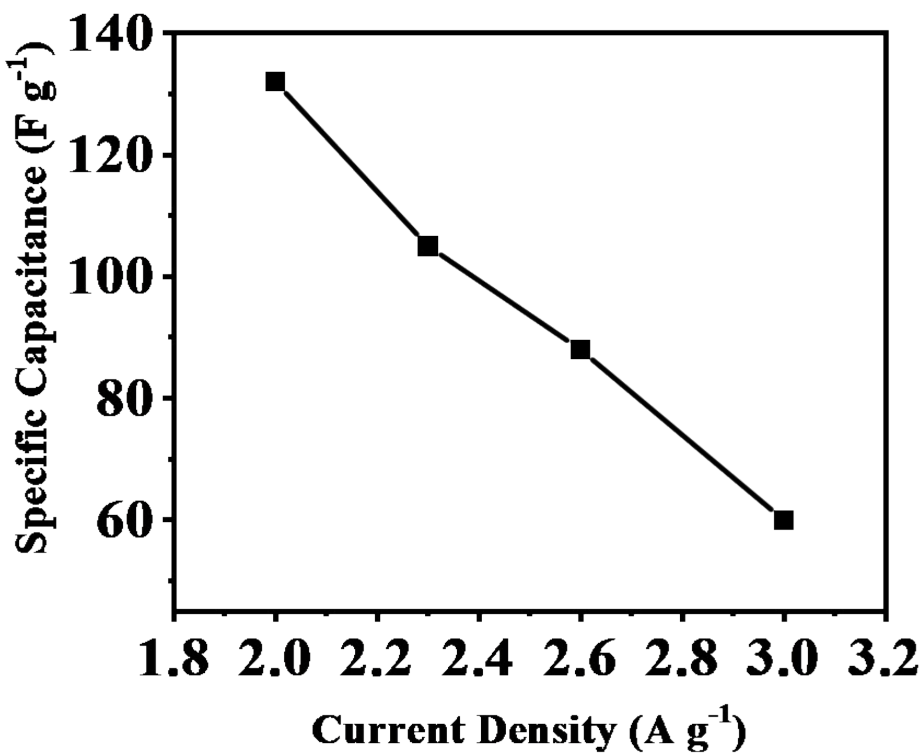

Fig. S8 Specific capacitance vs Current density plot of **Ni-BTC@ZIF-67** device.

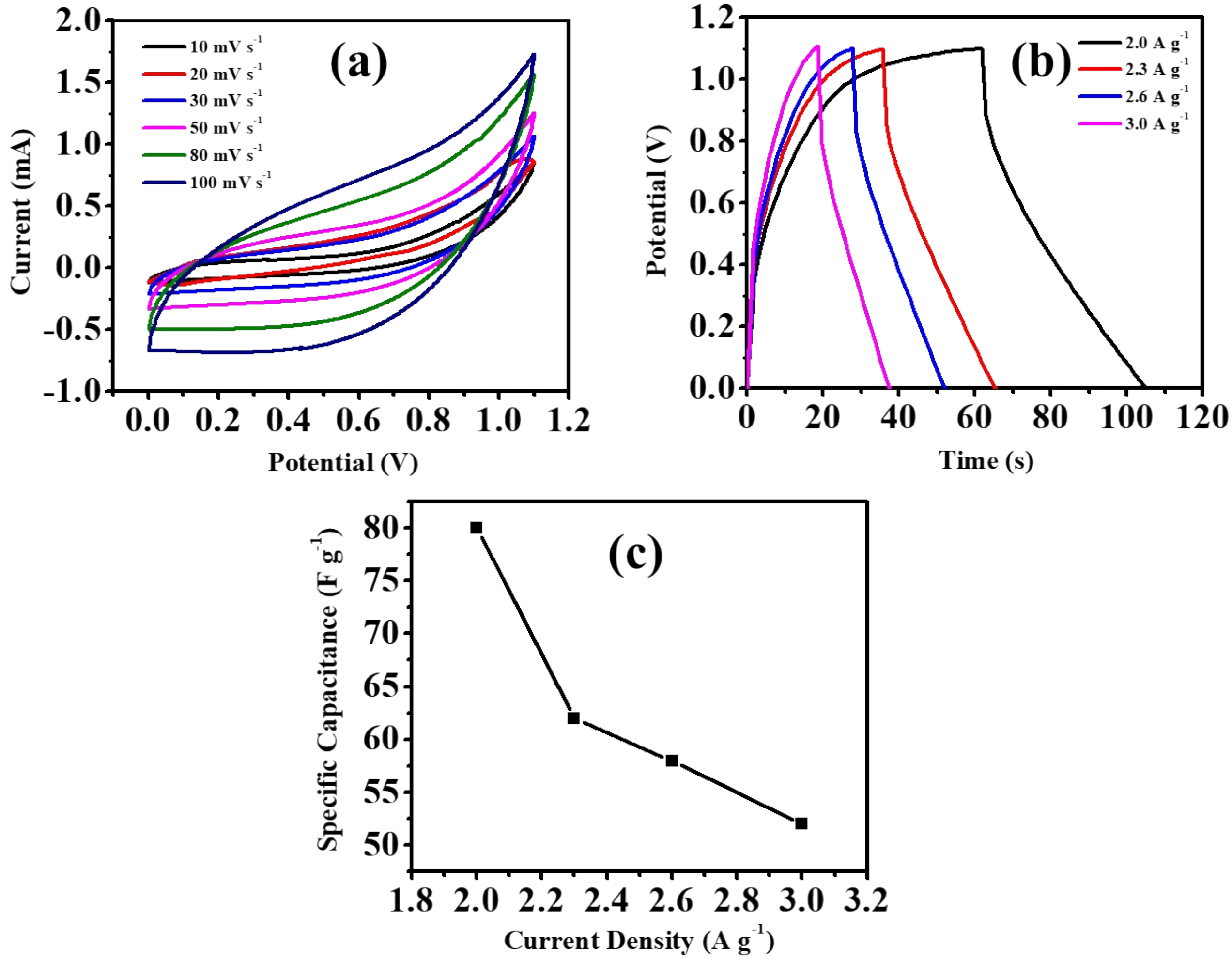

Fig. S9 (a-b) CV and GCD plot at several scan rates and current densities, respectively, and (c) Specific capacitance Vs. current density curve of **Ni-BTC** device.

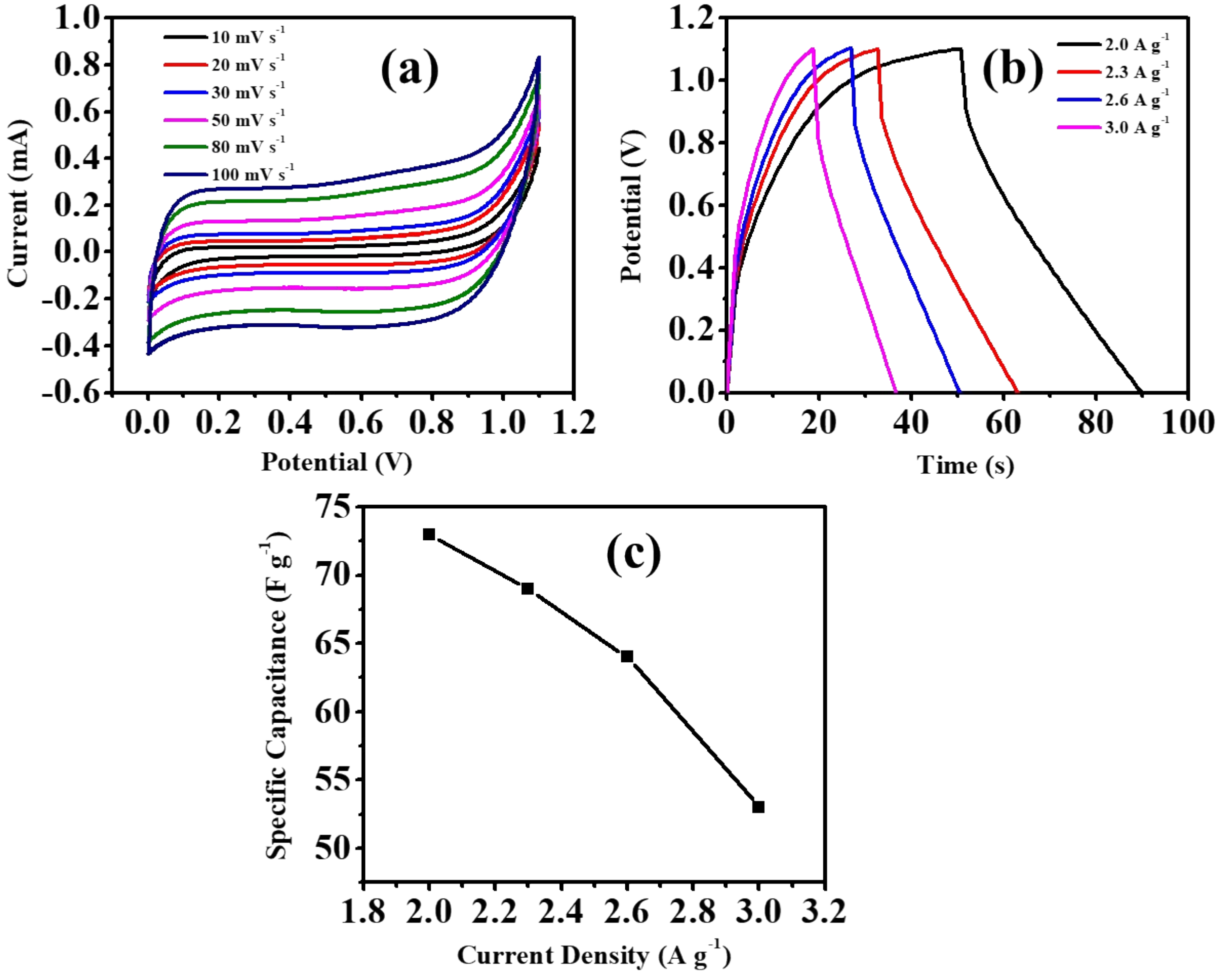

Fig. S10 (a-b) CV and GCD plot at several scan rates and current densities, respectively, and (c) Specific capacitance Vs. current density curve of **ZIF-67** device.

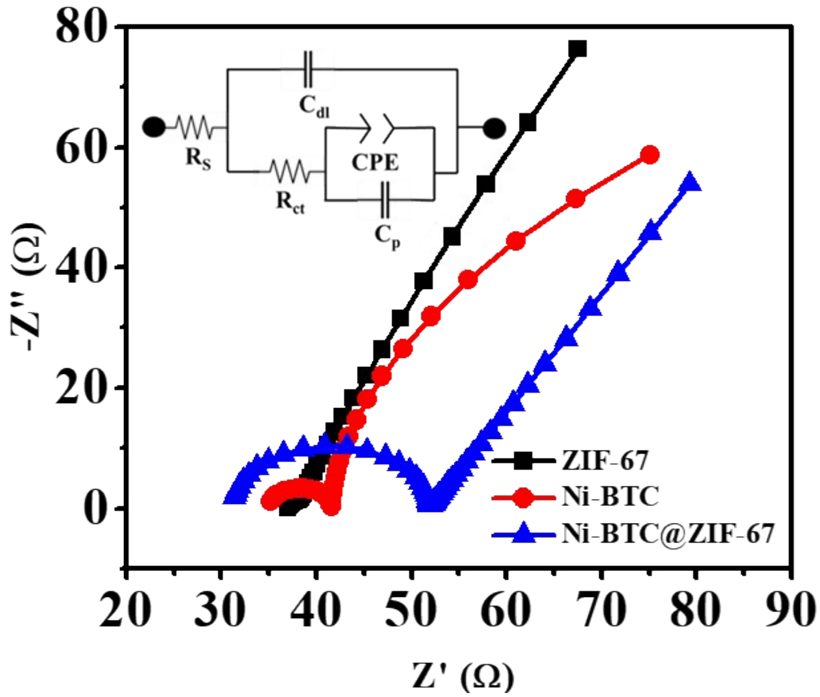

Fig. S11. Nyquist plot for **Ni-BTC@ZIF-67**, Ni-BTC, ZIF-67 device.

Table S1 Comparative BET surface area

Name	**Surface Area (m^2/g)**	**Pore radius (nm)**
ZIF-67	1903.812	0.8547
Ni-BTC	75.289	1.9206
Ni-BTC@ZIF-67	746.987	0.8599

Table S2 Circuit fitting parameter of Nyquist plot for three-electrode system.

Element	**ZIF-67**	**Ni-BTC**	**Ni-BTC@ZIF-67**
R_S (Ω)	13.2	12.9	9.57
R_{ct} (Ω)	6.77	8.86	3.60
C_{dl} (μF)	6.18	7.41	13.4
Q (nMho*s^N)	23.3 (N= 0.413)	22.3 (N=0.435)	25.5 (N= 0.47)
C_p (μF)	34.5	33	26.8

Table S3 Circuit fitting parameter for the device.

Element	**Device of Ni-BTC@ZIF-67**	**Ni-BTC**	**ZIF-67**
R_S (Ω)	31.2	35.0	37.0
R_{ct} (Ω)	20.6	6.56	2.18
CPE (mMho*s^N)	5.37 (N= 0.7)	5.56 (N= 0.263)	3.47 (N= 0.669)
C_{dl}	82.3 (nF)	1.35 (µF)	315 (µF)
C_p	900 (fF)	2.43 (mF)	675 (µF)

References

1 R. Deka, V. Kumar, R. Rajak and S. M. Mobin, *Sustain Energy Fuels*, 2022, **6**, 3014–3024.

2 V. Kumar and H. S. Panda, *New Journal of Chemistry*, 2021, **45**, 5399–5409.